

1 **Know before you go: Data-driven beach water quality forecasting**

2

3 Ryan T. Searcy<sup>1</sup>, Alexandria B. Boehm<sup>1\*</sup>

4

5 1. Department of Civil & Environmental Engineering, Stanford University, 473 Via Ortega,

6 Stanford, CA, USA, 94305

7 \* Corresponding author: 473 Via Ortega, Room 189, Stanford, CA 94305,

8 [aboehm@stanford.edu](mailto:aboehm@stanford.edu)

9

10 **Abstract**

11 Forecasting environmental hazards is critical in preventing or building resilience to their impacts  
12 on human communities and ecosystems. Environmental data science is an emerging field that  
13 can be harnessed for forecasting, yet more work is needed to develop methodologies that can  
14 leverage increasingly large and complex datasets for decision support. Here we design a data-  
15 driven framework that can, for the first time, forecast bacterial standard exceedances at marine  
16 beaches with three days lead time. Using historical datasets collected at two California sites, we  
17 train nearly 400 forecast models using statistical and machine learning techniques and test  
18 forecasts against predictions from both a naive ‘persistence’ model and a baseline nowcast  
19 model. Overall, forecast models are found to have similar sensitivities and specificities to the  
20 persistence model, but significantly higher areas under the ROC curve (a metric distinguishing a  
21 model’s ability to effectively parse classes across decision thresholds), suggesting forecasts can  
22 provide enhanced information beyond past observations alone. Forecast model performance at  
23 all lead times was similar to that of nowcast models. Together, results suggest that integrating  
24 the forecasting framework developed in this study into beach management programs can  
25 enable better public notification and aid in proactive pollution and health risk management.

26

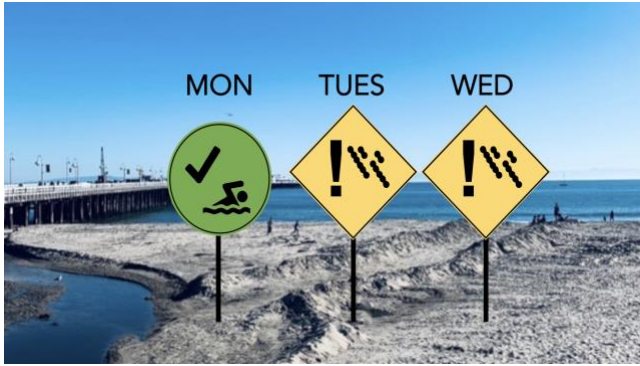
27 **Keywords:** data-driven models, water quality forecasting, machine learning

28

29 **Synopsis:** New environmental data science methodologies are needed to improve  
30 environmental hazard prediction. This study presents a framework to forecast regulatory  
31 exceedances of fecal indicator bacteria with three days lead time.

32

33 TOC Art:



34

35

## 36 **Introduction**

37 Environmental hazards including earthquakes, heat waves, wildfires, disease outbreaks, and  
38 acute water pollution threaten ecosystems and human communities around the planet. For  
39 example, it is estimated that weather- and climate-related disasters in the US have been  
40 responsible for more than 9,000 deaths and costs greater than \$1.8 trillion since the year 2000.<sup>1</sup>  
41 Forecasting these events is important to better enable disaster mitigation and resilience, but is  
42 often difficult to do accurately due to the rare and complex nature of these events.<sup>2,3</sup>

43         One challenge of hazard forecasting relates to the heterogeneity of environmental  
44 systems. It is difficult to predict the frequency and strength of hazards because they are  
45 functions of the interaction of multiple natural phenomena; they often vary in space in different  
46 regions of the planet; and they can change over time (especially as climate change and  
47 anthropogenic impacts accelerate).<sup>2,4</sup> Perhaps resulting from this heterogeneity, many ways of  
48 issuing environmental forecasts have been developed ranging from completely non-technical  
49 (such as using animal behavior to forecast earthquakes<sup>5</sup>) to entirely computational (such as  
50 global climate models that require the use of supercomputers).

51         Another barrier to effective forecasting relates to the nature of the data representing  
52 environmental systems which are often available from multiple sources in multiple spatial and  
53 temporal resolutions; noisy and sparse due to the difficulty in data collection (particularly for  
54 biological parameters); and skewed due to the rarity of events. Data-driven techniques - which  
55 take advantage of statistical and algorithmical relationships amongst datasets and are the  
56 primary tools of the emerging field of *environmental data science* - can be effective in extracting  
57 meaning from complex data.<sup>4</sup> Particularly, environmental data science is well-equipped to  
58 leverage the increasingly large and more real-time environmental datasets that are available  
59 from sources such as remote sensing platforms,<sup>6,7</sup> ecosystem monitoring stations,<sup>8,9</sup> individual

60 sampling campaigns, and model output.<sup>10,11</sup> As a result, data-driven hazard forecasting  
61 applications previously documented include predicting flooding,<sup>12</sup> air pollution,<sup>13</sup> foreign species  
62 invasion,<sup>14</sup> and harmful algal blooms.<sup>15,16</sup>

63         However, new and enhanced methodologies are still needed for data-driven  
64 environmental forecasts to have broad application. This is partially due to the unique complexity  
65 of environmental data which provides a barrier to using methods that have been successful in  
66 forecasting applications in other fields. For example, time series analysis techniques such as  
67 ARIMA have been successfully used for predicting financial outcomes but can break down when  
68 applied to environmental time series that are heavily-skewed (as is the case with rare event  
69 prediction) or unevenly spaced.<sup>17</sup> Developing new methods for specific environmental data  
70 science problems will improve the translation of complex datasets and subsequently improve  
71 decision support for environmental management.<sup>4</sup>

72         A specific opportunity to enhance environmental data science methodology is in the  
73 management of recreational beach water quality. At beaches around the planet, fecal indicator  
74 bacteria (FIB) - organisms that can be indicative of the presence of enteric pathogens - are  
75 monitored in water. However, FIB monitoring is often conducted infrequently (e.g. weekly or less  
76 often)<sup>18</sup> and relies on laboratory methods that delay result availability 24-48 hours; thus, beach  
77 management decisions and subsequent public notification often do not reflect current water  
78 quality conditions.<sup>19</sup> To augment monitoring, data-driven models have been used previously to  
79 predict FIB standard exceedances at beaches.<sup>20-22</sup> FIB models are often regression- or machine  
80 learning-based, and use environmental observations like tide, wave, and meteorological  
81 parameters as inputs to make predictions. Models can be more sensitive than the 'persistence  
82 method' of using a single day-old measurement to represent water quality<sup>23,24</sup> and can provide  
83 more frequent information to beach managers and beachgoers than sampling alone.<sup>25</sup>

84         Though often referred to as providing water quality 'forecasts',<sup>26-28</sup> most models are  
85 designed to issue FIB 'nowcasts'; technically, model outputs are near real-time predictions of

86 current water quality conditions rather than true forecasts which are predictions of future  
87 conditions. Nowcasts have limited use because in cases where water quality is predicted to be  
88 poor, same-day predictions give managers only a few hours to conduct adaptive sampling and  
89 make beach management decisions. Water quality forecasts – or predictions of water quality  
90 issued one or more days in advance – could alleviate these limitations, allowing for more  
91 effective beach management from local agencies as well as providing beachgoers more time to  
92 decide where to recreate based on water quality.

93 Few studies have investigated FIB forecasting. Frick et al.<sup>29</sup> converted a linear  
94 regression-based nowcast model developed for Lake Erie to provide forecasts for one day in the  
95 future. To do this, they substituted observed model variables with their forecast versions as  
96 model inputs. Zhang et al.<sup>30</sup> used wavelet analysis and neural networks to forecast FIB in Lake  
97 Michigan up to 24 hours in advance without using independent environmental variables. Both  
98 studies focus on lacustrine beaches with forecast lead times (the hours or days between when a  
99 prediction is issued and when it is valid) of one day or less. While there are examples of  
100 forecasting other beach parameters days in advance (such as tide level, harmful algal blooms,  
101 and air quality),<sup>7,31,32</sup> to our knowledge no work exists testing FIB forecasts at marine beaches.

102 The objective of the present study is to develop and test a data-driven framework that  
103 can effectively forecast FIB at marine beaches up to three days in advance. Our approach is  
104 based on methodology that is commonly applied in the development of nowcast models,  
105 including using a standard data science ‘pipeline’ (or workflow) to develop models and applying  
106 well-studied regression and machine learning model types. However, a key difference between  
107 nowcast methodology and our framework is that model inputs are intentionally limited to  
108 environmental observations made at least the number of days in advance of the time for which  
109 the FIB forecast is made. This means that as forecast lead time increases, the larger the gap in  
110 time between FIB and the observed model inputs. This approach is supported by knowledge

111 that predictive information can be found in environmental observation temporally lagged from an  
112 FIB observation.<sup>33,34</sup>

113         Using forecasting datasets composed of historical observations of FIB and  
114 environmental data, we apply a custom data science workflow to develop a series of machine  
115 learning models for two California marine beaches. We evaluate the models' ability to forecast  
116 FIB standard exceedances for one, two, and three days lead time, and assess the most  
117 common environmental parameters for each time step. We compare forecast performance to  
118 that of both naive models and of baseline nowcast models. The results of this work will allow  
119 practitioners to extend beyond nowcasting applications to make FIB predictions days in  
120 advance. Further, this work serves as a foundation that can be built upon with future work to  
121 improve forecasting of poor beach water quality as well other environmental hazards.

## 122 **Methodology**

### 123 **Study Sites**

124 Two California marine beaches were chosen for the study: Cowell Beach (CB, 36.962 N,  
125 122.023 W) and Huntington State Beach (HSB, 33.633 N, 117.966 W) (Figure S1). Both sites  
126 have a Mediterranean climate in which most precipitation events occur between the months of  
127 November and March. Sites were selected based on popularity with beachgoers, historical data  
128 availability, and differences in geomorphology, climate, and water quality conditions; a detailed  
129 description of the sites including notes on recent infrastructure changes can be found in the  
130 Supporting Information.

131

### 132 **FIB and Environmental Data**

#### 133 **FIB Data**

134 FIB monitoring is conducted year-round at both sites; a description of monitoring methodology  
135 can be found in the SI. *Escherichia coli* (EC) and Enterococcus (ENT) data were collated from a

136 State of California online database (<http://ceden.org/index.shtml>). Samples collected during the  
137 summer months (April-October) between 2007 and 2021 were used in this analysis. Beach  
138 sampling occurred approximately weekly at CB and twice weekly at HSB; no significant serial  
139 correlation was found in these datasets. Samples measured below the limit of quantification  
140 (LOQ) were flagged and assigned a value of ½ the LOQ. FIB samples with concentration in  
141 exceedance of the State of California’s regulatory standard (104 and 400 CFU/100 ml for EC  
142 and ENT samples, respectively)<sup>35</sup> were also flagged.

143

#### 144 **Environmental Data**

145 Historical environmental data were compiled for each beach from internet sources through  
146 manual download or API access; specific station details (including the sampling interval for each  
147 data type) are provided in Table S1. Oceanic data include tide, wave, and water quality  
148 parameters. Tide level predictions based on harmonic constants were available from the  
149 National Oceanic and Atmospheric Administration (NOAA). We used tidal predictions as  
150 opposed to observations because tides can be forecast accurately years in advance and NOAA  
151 maintains a historical archive of tide predictions (which is required for forecast model training,  
152 see below)<sup>36</sup>. Wave parameters including significant wave height, average wave period, and  
153 dominant wave period were measured by regional buoys maintained by the Coastal Data  
154 Information Program (CDIP). These buoys also collected water temperature data. Other water  
155 quality parameters such as chlorophyll, turbidity, dissolved oxygen, pH, salinity, and conductivity  
156 were measured by automated pier-based stations maintained by the Central and Northern  
157 California Ocean Observing System (CenCOOS).

158 Meteorological data include air and dew point temperatures; wind speed and directions;  
159 precipitation totals; and solar irradiance. These parameters were aggregated from multiple  
160 meteorological stations maintained by the National Climatic Data Center (NCDC), the California  
161 Irrigation Management Information System (CIMIS), and CenCOOS. Stream discharge data

162 collected from automated USGS gauges located in the San Lorenzo River and Santa Ana River  
163 were used in CB and HSB analyses, respectively. Finally, alongshore and crossshore current  
164 velocities measured by high-frequency radar maintained by CenCOOS were used in HSB  
165 analyses. All data sources provide quality assurance information on their websites to verify data  
166 veracity.

167

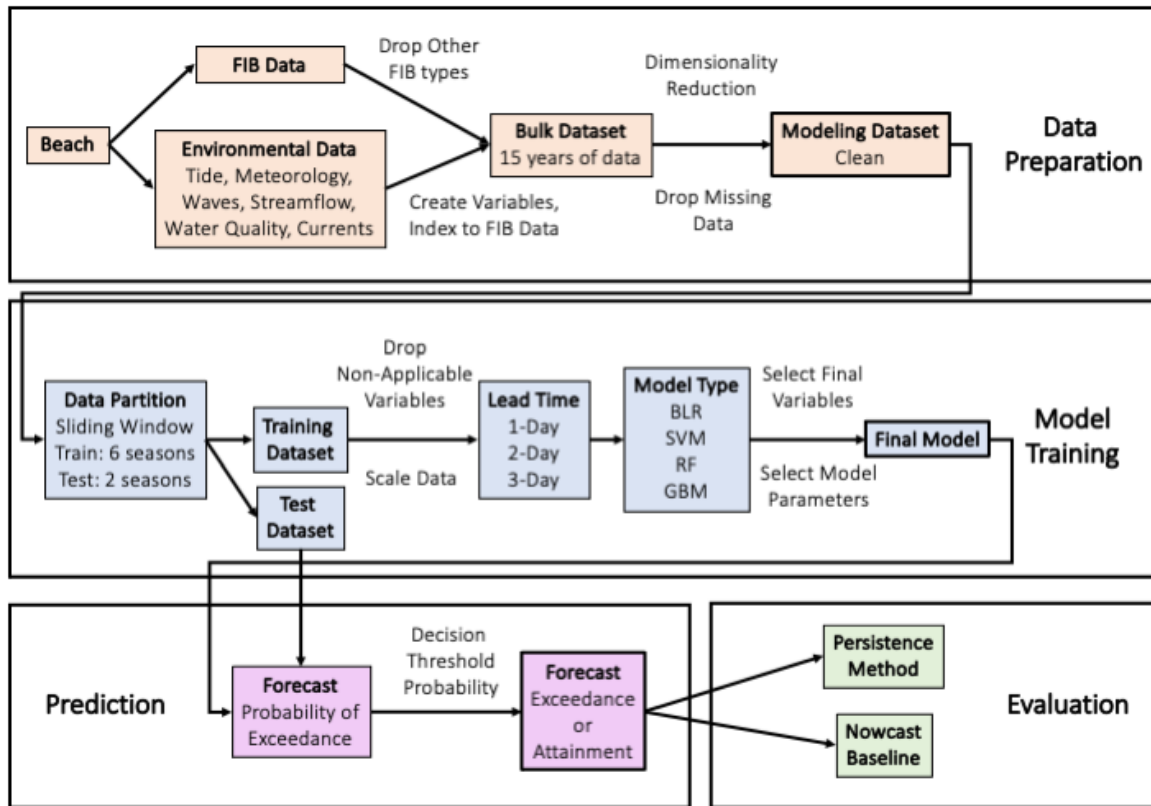
## 168 **Forecast Modeling**

### 169 **Overview**

170 We developed a suite of models that can forecast up to three days in advance whether FIB  
171 concentrations at a given beach will exceed regulatory standards based on the input of  
172 environmental variables. Rather than a single model that could at once forecast FIB at all times  
173 in the future, FIB forecasts were made by three individual models each developed to predict FIB  
174 on a specific day in the future. The following terminology and notation will be used henceforth to  
175 describe forecast models. The time upon which a prediction is output by a model is the *forecast*  
176 *issue time*, while the time in the future for which a forecast is made is the *forecast validity time*.  
177 The difference between the forecast issue and validity times is the *forecast lead time*. In this  
178 study, the forecast validity time (i.e. the time for which a forecast is made) will be assigned a  
179 timestamp  $t = 0$ . It then follows that a forecast of lead time  $L$  is issued by the model on  $t = -L$   
180 where the units of  $L$  are days. This frame of reference enables consistency when organizing  
181 modeling datasets for models of varying lead times, and is equivalent to a frame of reference  
182 where forecast issuance (rather than validity) occurs at  $t = 0$ . For example, using variables  
183 observed prior to  $t = -3$  to issue a forecast for  $t = 0$  (i.e. a three day lead time) is equivalent to a  
184 forecast valid at  $t = 3$  issued by a model with input variables observed prior to  $t = 0$ .

185 Model development included aggregating FIB and environmental variables into bulk  
186 datasets, pre-processing bulk modeling datasets by reducing dimensionality and removing  
187 missing values; partitioning data into training and test datasets; selecting the final model

188 variables; and fitting and evaluating the predictive model (Figure 1). This process was followed  
 189 for each model developed for a given beach, FIB type, data partition, forecast lead time, and  
 190 model type. Model development was performed using the Python programming language and  
 191 specifically using the *scikit-learn* machine learning package.<sup>37</sup>



192  
 193 Figure 1: Flow diagram of the development of an individual forecast model. Procedure is repeated for  
 194 each beach, FIB type, data partition, lead time, and model type.

196 **Modeling Datasets**

197 Bulk modeling datasets for a given beach were composed of historical FIB observations  
 198 (dependent variable) and environmental (independent) variables. Environmental variables were  
 199 created by time indexing raw data to each FIB observation at a given beach. Because the  
 200 temporal resolution of the FIB datasets are on the order of days, raw environmental data with  
 201 higher frequency sampling resolution were transformed into bulk daily statistics (e.g. daily

202 maximum tide level, daily mean significant wave height, the sum of precipitation over the  
203 previous seven days). Categorical variables were created by grouping by environmental  
204 condition on a given day. Such categorizations include whether there was spring or neap tide;  
205 during periods of discrete wind and current directions (offshore or onshore and upshore or  
206 downshore); and when wind speed, significant wave height, dominant wave period, chlorophyll,  
207 and turbidity were above or below their historical 75th percentile (which served to indicate  
208 relatively elevated levels of the condition).

209 Temporally lagged variables were created by employing a temporal shift of up to 7 days  
210 between environmental variables and FIB observations. Examples include mean air  
211 temperature observed two days prior, dichotomized wind conditions observed four days prior,  
212 and total precipitation observed between three and seven days prior. While lagged variables  
213 have been shown to significantly improve the predictive performance of FIB nowcast models,<sup>33</sup>  
214 they are necessary in this work primarily because of operational constraints specific to  
215 forecasting; that is, only environmental observations made on or before the forecast issuance  
216 time (which lags from the forecast validity time) can be used. The exception to this were tidal  
217 parameters. The instantaneous tide level at the time of FIB sampling was also used as a model  
218 variable because this variable is available for operational FIB forecasting as tide data were  
219 forecasts themselves.

220 In addition to the aforementioned environmental categorizations, we created variables  
221 that indicated the month of sample collection and whether samples were collected on  
222 weekends. Precipitation, streamflow, chlorophyll, and turbidity parameters were  $\log_{10}+1$   
223 transformed (i.e.  $\log_{10}$ -transformed after adding 1) to reduce skew. Finally, we chose not to  
224 include autoregressive FIB variables (e.g. the most recent FIB measurement) as independent  
225 variables due to the unevenly spaced FIB time series available at the study beaches. A  
226 maximum of 266 environmental variables spanning seven types (meteorological, tide, wave,  
227 water quality, streamflow, current, and date) were included in bulk modeling datasets (Table

228 S2.1 - 2.7). It should again be emphasized that all environmental variables except for tide  
229 variables were composed of measured data as opposed to forecast (or modeled) data; this is  
230 primarily due to poor availability of forecast environmental data. All data used in this study are  
231 available in the Stanford Digital Repository and can be accessed at  
232 <https://purl.stanford.edu/nw799cp6263>.<sup>38</sup>

233 The bulk datasets represent an aggregation of data from multiple sources and a range of  
234 temporal lags, and thus often contained hundreds of modeling variables and included missing  
235 data points. Pre-processing was required prior to individual model development in order to  
236 reduce the likelihood of overfitting (which can occur when training models on a large number of  
237 variables) and to yield clean modeling datasets.

238 Dataset dimensionality was performed by first removing irrelevant variables from the  
239 bulk modeling datasets. This included zero-variance variables, variables related to observations  
240 of FIB of the other type (i.e. EC and ENT were modeled independently), and variables (except  
241 for tidal) representing data observed on the same day of an FIB observation as they are often  
242 not available for use operationally in a forecast model. To further reduce dataset dimensionality  
243 as well as multicollinearity, highly correlated environmental variables (Spearman Rank  
244 Correlation > 0.9) were identified and the variable of the pair with the lowest magnitude  
245 Spearman correlation with FIB concentrations were dropped from the dataset. Remaining  
246 variables with a number of missing data points greater than 15% of the total length of the  
247 dataset were dropped. A threshold of 15% was selected because we found it balanced dataset  
248 length (i.e. number of observations available for model training and testing) and maximizing the  
249 total number of the variables available for inclusion in models. Finally, if missing values  
250 remained, the entire record for those time points (i.e. the FIB observation and the environmental  
251 variables indexed to it) was omitted from the modeling data set. We chose not to employ  
252 imputation because there were often large gaps in the environmental variable datasets (i.e.  
253 spanning seasons) in which imputation could not be useful. Further, dropping missing values did

254 not significantly reduce the number of data points available for model training and testing (i.e. at  
255 least 85% of datapoints maintained. These steps yielded a clean modeling dataset specific to a  
256 given beach and FIB type that enabled consistency when developing models of varying lead  
257 times.

258

### 259 **Data Partitioning**

260 Modeling datasets were partitioned into training and test datasets. Six consecutive summer  
261 seasons of data were included in the training datasets which were used to select final modeling  
262 variables and parameters and fit models. The subsequent 2 seasons of data composed the test  
263 datasets which were used to evaluate predictive performance of the forecasts.

264 Multiple data partitions were created using a sliding window with a step of one year over  
265 the range of the entire modeling dataset. For example, if one partition included a training  
266 dataset with data collected between 2007 - 2012 and a test dataset with data collected during  
267 2013 and 2014, the following partition would entail a training dataset with data collected  
268 between 2008 - 2013 and a test dataset with data collected during 2014 and 2015. Thus, 8 total  
269 data partitions per modeling dataset were available.

270 Environmental variables were subsequently standardized in order to optimize model  
271 training. Variables were first centered by subtracting the variable's mean value and  
272 subsequently scaled by dividing by the variable's variance. The means and variances from the  
273 partition's training dataset were used to standardize the data in both the training and test  
274 datasets.

275

### 276 **Forecast Model Training**

277 The data of each partition were subsequently used to develop models for all three forecast lead  
278 times as well as baseline nowcast models. Prior to training forecast models of a given lead time,  
279 a final removal of environmental variables (with the exception of tide variables which are

280 technically available for all lead times because they are composed of forecast data) was  
281 conducted such that the models were fit only on data available for operational use. For example,  
282 total observed precipitation on  $t = -2$  is available for use in nowcast (lead time of 0) and 1-day  
283 forecast models, but is operationally unavailable for 2- and 3-day forecast models. This final  
284 removal led to an increasingly smaller number of variables available for model training as lead  
285 time increased.

286 Models were trained as binary classifiers. Predictions were made in two-steps: first  
287 outputting the probability of whether FIB concentrations were in exceedance of the water quality  
288 regulatory standard, and then converting that probability to either the positive class (i.e. FIB  
289 standard exceedance) or negative class (i.e. attainment or 'non-exceedance' of FIB standard)  
290 based on if it was above or equal to or below the decision threshold probability, respectively.  
291 The default decision threshold probability used was 0.5.

292 We trained four models for each forecast lead time using the following statistical and  
293 machine learning model types: binary logistic regression, support vector machine, random  
294 forest, and gradient boosted machine. Each model type is available in the *scikit-learn* package  
295 in Python, and has been used previously to predict FIB or other water quality parameters.<sup>39–42</sup>  
296 Binary logistic regression (BLR) is a statistical model that has an interpretable relationship  
297 between environmental variables and predicted FIB. We used a BLR model with an 'elastic net'  
298 penalty. Support vector machine (SVM) is a model that employs kernel functions which  
299 nonlinearly map data such that the hyperplane that separates predicted classes is optimized.  
300 Random forest (RF) is an ensemble model where the prediction is an aggregate of the  
301 predictions of multiple decision 'trees'. Gradient boosted machine (GBM) is similar to RF in that  
302 multiple weak estimators are fit as an ensemble; however, each subsequent tree fit is 'boosted'  
303 by learning the error resulting from the previous. Default model parameters are listed in Table  
304 S3.

305 Models were trained using a process that used cross-validation to first select final model  
306 variables from the full training dataset and then optimize model parameters from the training  
307 datasets. Balanced accuracy (the mean of model sensitivity and specificity, defined below) was  
308 used as the cross-validation score metric in all steps of this process. Variable selection involved  
309 a two-step process. The first step further reduced the dimension of the training dataset by using  
310 the *permutation feature importance* algorithm in the *scikit-learn* package.<sup>37</sup> The permutation  
311 feature importance (PFI) of a given variable is indicative of how dependent a model is on that  
312 variable and is calculated as the change in model score metric upon training a model after  
313 randomly shuffling the variable's data. Each variable was shuffled five times, and the mean PFI  
314 resulting from the shuffling was calculated. Variables with mean PFI less than 1.5 times the  
315 grand mean PFI of the entire variable set were dropped from the training dataset. A value of 1.5  
316 was selected because it was found to balance model training time and variety for subsequent  
317 variable selection.<sup>43</sup>

318 The second step in variable selection was a recursive feature elimination algorithm with  
319 cross-validation. The training dataset was first split into five 'folds' or subsets, four of which were  
320 used to fit submodels and the remaining used to cross-validate the submodel's score. In a  
321 stepwise manner, the algorithm dropped the one variable from the dataset such that the  
322 submodel score (i.e. balanced accuracy) on the validation data is maximized. Variable removal  
323 was repeated until the minimum number of submodel variables remained (for this study, we set  
324 this parameter to 3). The entire stepwise process was repeated five times using all  
325 combinations of data folds for submodel fitting and validation. Upon completion, the set of  
326 variables corresponding to the highest average cross-validation score was selected as the final  
327 modeling variable set.

328 A grid search algorithm with cross-validation was then used to optimize the model  
329 parameters specific to the given model type. Similarly to recursive feature elimination, grid  
330 search involved splitting the training dataset into five folds, fitting submodels with varying model

331 parameters on four folds, and evaluating the model score on the fifth. The procedure was  
332 repeated until all combinations of model parameters were exhausted. The parameters used in  
333 the search for each model type are listed in Table S3. The entire parameter search was  
334 repeated a total of five times exhausting all combinations of data folds for submodel fitting and  
335 validation. The model with parameters that maximized the average cross-validation score  
336 averaged over the submodels was used as the final model.

337

### 338 **Forecast Evaluation**

339 The test datasets were used to evaluate the predictive performance of models. This was done  
340 by running models to output forecasts of whether FIB exceeded regulatory standards, and  
341 comparing predictions to FIB measurements. Three performance metrics were used to evaluate  
342 models: sensitivity, specificity, and area under the receiver operating characteristic curve.

343 *Sensitivity* is defined as the proportion of positive values (i.e. FIB standard exceedances)  
344 correctly predicted by the model; models with higher sensitivity are more health protective.

345 *Specificity* is defined as the proportion of negative values (i.e. FIB in attainment of the standard)  
346 correctly predicted. It is valuable to consider both sensitivity and specificity because beach  
347 managers typically desire models to be effective in predicting both days of FIB standard  
348 exceedances and attainment. *Area under the receiver operating characteristic curve (AUC)* is a

349 bulk metric that integrates sensitivity and specificity across a range of potential decision  
350 threshold probabilities, and is less biased than those metrics when comparing performance  
351 between models tested on datasets with differing proportions of FIB standard exceedances.<sup>21,44</sup>

352 AUC ranges from 0 to 1, with a value of greater than 0.5 indicating that a model's predictive  
353 ability is greater than guessing at random and a value of 1 indicating perfect delineation of  
354 positive and negative classes. Aggregate performance was calculated across all developed  
355 models, by individual model type, and for all models developed for a given beach and FIB type.

356 Model performance was contextualized by comparing these metrics to those calculated  
357 for the 'persistence method', a naive model which assumes the forecast FIB condition at a  
358 beach is equivalent to that indicated by the most recently collected observation prior to forecast  
359 issuance. The persistence method is the means by which beach management in California is  
360 currently conducted, and thus serves as a practical baseline to evaluate model performance.

361 Finally, performance metrics for forecast models were also compared to those calculated  
362 for nowcast models (lead time of 0) developed for the same data partition and model type. This  
363 allowed for evaluation on how forecasts of increasing lead time compared to the nowcast  
364 baseline on the same data.

365

## 366 **Results**

### 367 **FIB and Environmental Data**

368 Bulk modeling datasets for each beach were composed of FIB and environmental data collected  
369 over 15 summer seasons (April through October from 2007 - 2021) (Table S4). HSB had a  
370 higher proportion of samples measured below the LOQ (66% and 61% of EC and ENT samples,  
371 respectively) than CB (8% and 43%). Of the two FIB types considered in this study, EC  
372 exceeded the regulatory standard most frequently at CB (19% of all samples) while ENT  
373 exceeded most frequently at HSB (8%).

374

### 375 **Forecast Model Development**

376 The proportion of FIB exceedances varied between training and test datasets within partitions  
377 and between individual partitions, reflecting changing FIB distributions over the years (Table  
378 S5). The average proportion of FIB exceedances at CB (13% and 11% for EC and ENT test  
379 datasets, respectively) was higher than that for HSB (4% and 8%).

380 Across all combinations of beach, FIB type, dataset partition, forecast lead time, and  
381 model type, we developed 384 total forecast models. An additional 128 nowcast models were  
382 developed for baseline comparison.

383 A total of 130 unique variables across all models trained were selected through the  
384 variable selection process. The most common variable types selected in fitting forecast models  
385 were meteorological (appearing in 97% of models), tide (91%), and wave (83%) variables, while  
386 currents and water quality variables were the least common (appearing in 0% and 17% of  
387 models, likely owing to the poor availability of their data). Instantaneous tide level was the most  
388 common individual variable selected, appearing in 43% of models. The most frequently selected  
389 variables for models developed for each beach and FIB are listed in Table S6.

390 The number of modeling variables selected differed by model type (Figure S2). RF and  
391 GBM tended to have fewer variables (mean of 7 and 9, respectively) than SVM and BLR (mean  
392 of 11 and 12). Across all forecast models, the mean number of selected variables in a model  
393 was 10 and the maximum was 38. The number of variables in individual forecast models tended  
394 to decrease with increasing model lead time, mostly due to the increasingly limited availability of  
395 variables to select from.

396

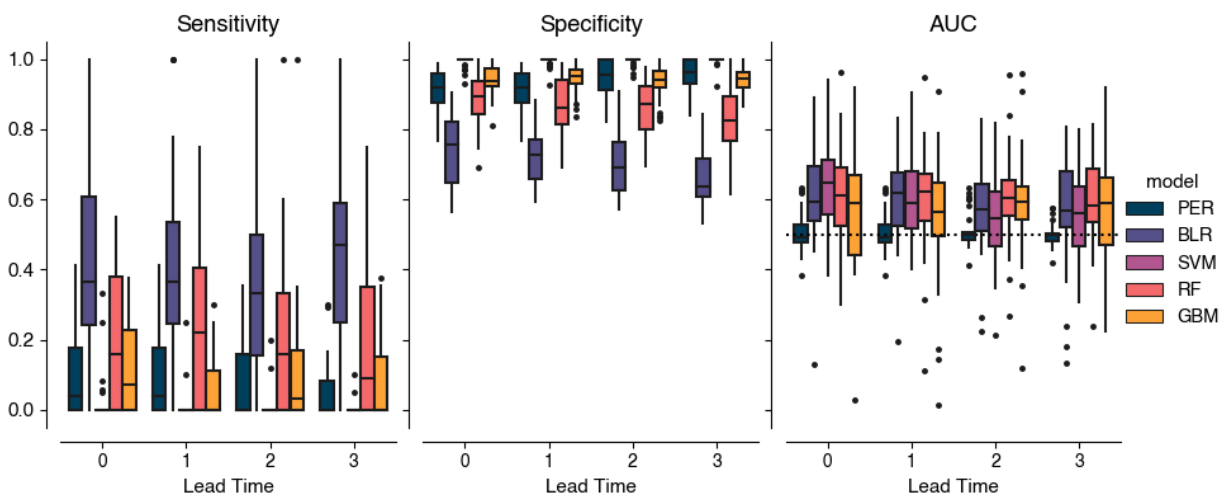
## 397 **Forecast Model Performance**

### 398 **Overall Performance**

399 FIB forecasts were made by running models on the test datasets and were compared to  
400 observations in order to evaluate predictive performance. Across all forecast models, median  
401 sensitivity was 0.00 (interquartile range (IQR) 0.00 - 0.31), median specificity was 0.92 (IQR  
402 0.77 - 0.97), and median AUC was 0.58 (IQR 0.50 - 0.66). The majority of forecast models we  
403 developed (76%) had AUC values greater than 0.5 (i.e. more informative than random  
404 guessing). Comparatively, the persistence method's median sensitivity was 0.00 (IQR 0.00 -  
405 0.15), median specificity was 0.95 (IQR 0.89 - 0.98), and median AUC was 0.50 (IQR 0.48 -

406 0.51). Further, the persistence method had 32% of instances with AUC greater than 0.5. At this  
407 aggregate level, forecast models do not appear to perform well in terms of sensitivity and  
408 specificity compared to the persistence model; however, we next disaggregate the results to  
409 investigate if specific models perform well.

410 Metrics grouped by individual model type showed that certain model types tended to  
411 outperform the persistence model (Figure 2, Table S7). Across all beaches, FIB types, data  
412 partitions, and lead time, the most sensitive model type was BLR (median of 0.40, IQR 0.22 -  
413 0.56) while the least sensitive was SVM (0.0, IQR 0.0 - 0.0). Specificity was highest for SVM  
414 models (1.00, IQR 1.00- 1.00), because all predictions were for the negative class. The next  
415 most specific model type was GBM (0.95, IQR 0.92 - 0.97); the lowest specificities came from  
416 BLR models (0.69, IQR 0.62 - 0.76). AUC was highest for RF (0.60, IQR 0.54 - 0.68) and lowest  
417 for SVM (0.56, IQR 0.48 - 0.65). BLR and RF were the model types with AUC most frequently  
418 greater than 0.5 (80% and 79% of models, respectively), while SVM was the least frequent  
419 (68%). No single model type was superior in all of the evaluation metrics, yet depending on the  
420 performance criteria of the end user (i.e. required sensitivity or specificity), each can be an  
421 effective model type for operational forecasting.



422  
423 Figure 2: Predictive performance of forecast models on test datasets. Model sensitivities, specificities,  
424 and AUC values are plotted in the left, middle, and right subplots, respectively. The dotted line in the AUC

425 subplot is set at a value of 0.5 for reference. Performance metrics are categorized by forecast lead time  
426 (x-axis). The lead time zero boxplots represent the results from the baseline nowcast models. Color  
427 indicates model type; PER corresponds to the persistence method. The middle line in the boxplots  
428 represents the median; the upper and lower edges of the boxes represent the 75th and 25th quantiles,  
429 respectively. The whiskers extend to 1.5 times the interquartile range (75th quartile–25th quartile).

430 Forecast models are developed specific to a given beach and FIB type, so we next  
431 aggregate performance metrics as such and show that forecast models perform well relative to  
432 the persistence method for beach management. For brevity, we present results below for EC at  
433 CB and ENT at HSB, yet metrics for all beach and FIB type groupings are listed in Table S8. For  
434 EC at CB, median sensitivity was 0.12 (IQR 0.0 - 0.34) for forecast models compared to 0.11  
435 (0.0 - 0.26) for the persistence method; median specificity was 0.91 (0.71 - 0.98) for forecast  
436 models and 0.90 (0.85 - 0.95) for the persistence method; and median AUC was 0.58 (0.48 -  
437 0.65) for models and 0.51 (0.47-0.58) for the persistence method. For ENT at HSB, median  
438 sensitivity was 0.10 (IQR 0.0 - 0.41) compared to 0.0 (0.0 - 0.0) for the persistence method;  
439 median specificity was 0.92 (0.77 - 0.99) for models and 0.97 (0.94 - 1.0) for the persistence  
440 method; and median AUC was 0.62 (0.56 - 0.70) and 0.50 (0.48-0.50) for the persistence  
441 method.

442

#### 443 **Comparison to Nowcast Models**

444 We developed 128 nowcast models using the same methodology described above for forecast  
445 models, but allowing for the inclusion of the most recently observed variables (i.e. from one day  
446 previous of prediction validity). Compared to persistence method predictions with a lead time of  
447 0, nowcast models had higher median sensitivity, specificity, and AUC (Table S9).

448 Overall, average predictive performance of nowcast models was similar to those of  
449 forecast models of all three forecast lead times. We assessed how performance changed  
450 between individual models of a given lead time and their associated baseline nowcast model (N

451 = 128 model comparisons per lead time). Model sensitivity decreased in a minority of forecast  
452 models (24%, 26%, and 27% for 1, 2, and 3 days lead time, respectively) relative to the  
453 associated nowcast model; forecast model sensitivity remained unchanged relative to nowcast  
454 for approximately half of forecast models of each lead time (likely an artifact of many models  
455 having sensitivities of 0.0). Model specificity decreased in 40%, 45%, and 45% of forecast  
456 models relative to the associated nowcast model for 1, 2, and 3 days lead time, respectively,  
457 while it increased in approximately one third of forecast models of each lead time respectively.  
458 Thus the median difference in specificity between forecast and nowcast models was 0.0 for all  
459 three lead times. Finally, forecast model AUC decreased in 59%, 57%, and 61% relative to  
460 nowcast models for 1, 2, and 3 days lead time, respectively; the median change in AUC was  
461 small (0.02, 0.02, and 0.04 for one, two, and three days lead time, respectively). Cumulatively,  
462 these results suggest that a comparable quality of information can be provided by forecast  
463 models as from their baseline nowcast models.

464

## 465 **Discussion**

466 We established an automated framework that can be used to develop data-driven models that  
467 forecast FIB at marine beaches for up to three days lead time. Our methodology extends  
468 beyond that used to develop FIB nowcast models by leveraging temporally-lagged  
469 environmental observations and multiple statistical and machine learning model types. We used  
470 the framework to train nearly 400 forecast models for two California beaches and tested their  
471 predictions against FIB observations. To our knowledge, this is the first demonstration that FIB  
472 levels at marine beaches can be predicted days in advance.

473 Our results show that forecast models can provide enhanced beach water quality  
474 information beyond single past observations alone (i.e. the persistence method). FIB  
475 concentrations tend to exhibit 'patchy' time series and can be heavily skewed, making them

476 difficult to predict with autoregressive techniques alone. Predictive models instead rely on  
477 observed environmental parameters which can be monitored more frequently than FIB and  
478 represent the physical, chemical and biological processes that control FIB fate and transport in  
479 the environment. Moreover, the statistical and machine learning models we considered in the  
480 framework have the potential to capture nonlinear relationships between FIB and environmental  
481 drivers.

482         An underlying design component specific to the forecasting framework is to utilize the  
483 knowledge that there is often a delayed effect between a given environmental driver (e.g.  
484 precipitation, wind-driven flow) and the expressed effect in FIB fate; this is represented in our  
485 framework through the use of lagged observed environmental variables. For example,  
486 precipitation observed six days prior was often included as a model variable, perhaps due to a  
487 six day gap between rainfall and contaminated runoff reaching the study site. Site-specific  
488 studies devoted to exploring FIB fate and transport mechanisms would be needed to verify this.

489         However, the effect of some environmental mechanisms on FIB fate can be more  
490 immediate (e.g. water temperature, solar irradiance).<sup>45-47</sup> Thus the presence of lagged  
491 environmental variables in models (which was more common as forecast lead time increased)  
492 may be more related to variable autocorrelation than a delayed effect on FIB. This may explain  
493 why solar irradiance observed four days prior was a frequently included parameter in models; if  
494 a parameter observed on or prior to forecast issuance is strongly correlated with its observation  
495 on the time of forecast validity  $t = L$ , then the lagged parameter acts more like a forecast  
496 variable.

497         It is interesting to note that instantaneous tide level - the single forecast variable used in  
498 this study - was the most often selected variable in FIB forecast models. Tide level is regarded  
499 as a parameter that can be forecast with high accuracy, and it has also been shown to be  
500 important in nowcast models developed previously at the study sites.<sup>25,43</sup> Future studies could  
501 examine the accuracy of forecasts of additional environmental parameters and the efficacy of

502 their inclusion as variables in forecast models. We expect precipitation forecasts could be  
503 beneficial model variables that may lead to improved model performance, especially during  
504 periods when precipitation occurs between forecast issuance and validity.. In this study we  
505 chose not to use forecast variables (aside from tide level) because model accuracy is affected  
506 by the accuracy of the forecast variables (as is evidenced by Frick et al.)<sup>29</sup> and historical records  
507 of forecast environmental parameters are often unavailable from the data source. However, a  
508 concerted effort to archive a sufficient number of environmental forecasts for model training  
509 could be made, or forecasts could be created using time series techniques.<sup>48</sup>

510 Predictive metrics of forecast models were similar to those of the comparative baseline  
511 nowcast models, suggesting that the predictive efficacy of a forecast modeling system can be  
512 maintained for at least three days. This result is somewhat surprising considering forecast  
513 accuracy of most environmental parameters is generally expected to decline with increasing  
514 lead time. That predictive metrics were similar between forecasts and nowcasts may further  
515 validate the notion that information predictive of FIB can be found in environmental observations  
516 collected less recently than solely the closest days to prediction validity. Future work could  
517 extend our framework to lead times of one week (or longer) to determine the lead times at which  
518 predictive efficacy drops significantly.

519 Despite frequently having improved performance over the persistence method, the  
520 sensitivities of forecast models (developed using the default decision threshold probability of  
521 0.5) were generally low (median of 0.0 overall, median of 0.4 for BLR models) and thus may be  
522 unacceptable for use for beach management where swimmer health protection is the priority.  
523 However, it should be noted that the status quo has even lower sensitivity than the forecast  
524 models. Low sensitivity could be due to a number of data limitations including site infrastructure  
525 changes which alter the FIB distributions between training and test sets, or lack of  
526 environmental data that truly explain FIB fate and transport at the site. An additional and likely  
527 limitation could be due to the imbalanced nature of the FIB datasets at the specific beaches we

528 tested, where many more samples were in attainment than in exceedance of the regulatory  
529 standard; this is evidenced by the poor performance of the persistence method. The effect of  
530 class imbalance on model sensitivity has been observed previously by Thoe et al. (2015).<sup>23</sup> To  
531 account for low default sensitivities, their group optimized their models by ‘tuning’ the decision  
532 threshold probability at which a prediction is for a positive or negative class on the training data.  
533 This increased the sensitivity of their BLR models on test data from 19% to 50%. When we  
534 tuned the decision threshold probabilities of a random subset of our models, we saw an  
535 improvement in sensitivity with a drop in specificity that would likely be acceptable for beach  
536 management<sup>25</sup> (see the Supporting Information for more details). However, because there is a  
537 tradeoff between model sensitivity and specificity, models should be tuned based on the risk  
538 tolerance of the forecast user.

539           Comparison of the AUC of our models to those in the literature show that forecast  
540 models (agnostic of tuning) can perform on par to what is already expected in the water quality  
541 prediction field. Our models (particularly, RF and GBM models) were able to distinguish  
542 between positive and negative classes similarly to those developed by Brooks et al. .<sup>21</sup> Over the  
543 15 nowcast model types they tested, the median AUC was 0.67 (IQR 0.63-0.71) which is similar  
544 to ours.

545           The framework presented here serves as a foundation for future beach water quality  
546 forecasting research and implementation. Additional potential research topics include assessing  
547 the effect of training dataset size (i.e. the number of observations) on model performance;  
548 exploring different model outputs like categorical or probabilistic predictions; testing deep  
549 learning model types such as long short-term memory neural networks (which was out of scope  
550 of the present study);<sup>12,16</sup> and incorporating more locally-collected environmental data as well as  
551 previous FIB observations as predictor variables (which may become operationally feasible with  
552 the onboarding of rapid<sup>49</sup> and autonomous<sup>50</sup> sampling methods that enable higher resolution  
553 datasets).

554           This framework can be employed by health agencies, community groups, or other beach  
555 water quality stakeholders who desire FIB forecasts up to three days in advance. With adequate  
556 support, the framework can also be integrated into existing nowcast modeling systems.  
557 Attention must be given to the time indexing of environmental data; specifically, we suggest  
558 organizing environmental variables such that forecast issuance occurs at  $t = 0$ . Many  
559 environmental data sources can be accessed via the internet, enabling the automation of  
560 modeling pipelines and the issuance of daily forecasts of all lead times simultaneously.  
561 Forecasts can be compared to routine monitoring data as they are collected, and models can be  
562 re-tuned or retrained based on what performance level is desired by operators. Further,  
563 forecasts could be used as a basis to conduct proactive sampling in the case that FIB  
564 exceedances are predicted. Thus, water quality forecasts would provide agencies and beach  
565 communities much more information than what sampling alone provides, leading to improved  
566 environmental awareness and management.

567           Though our framework was developed specifically for FIB prediction, we expect it may  
568 be useful for predicting other environmental hazards that have similarly structured and available  
569 data (such as harmful algal blooms or shellfish toxicity). We encourage the extension of this  
570 framework to other environmental prediction applications especially as the availability of unique  
571 environmental datasets and novel modeling types continues to grow. Developing new  
572 techniques or extending upon existing methodologies is an important step in advancing  
573 environmental data science and thus better understanding our interactions with the natural  
574 environment.

575

#### 576 **Data Availability Statement**

577 The data that support the findings of this study are openly available at the Stanford Digital  
578 Repository: <https://purl.stanford.edu/nw799cp6263>. The Python code used to manipulate data  
579 and develop and test models can be found at: <https://github.com/rtsearcy/wq-forecasting>

580

581 **Acknowledgements**

582 This study was supported by the University of Southern California Sea Grant Program, National  
583 Oceanic and Atmospheric Administration, U.S. Department of Commerce, under grant number  
584 NA18OAR4170075.

585

586 **Supporting Information:** Model tuning case study. List of environmental variables used for  
587 modeling and the stations from which data were acquired. Grid search parameters for each  
588 model type. Data partition summaries. Most frequent model variables. Predictive performance  
589 by model type and by beach.

590

591 **References**

- 592 (1) National Centers for Environmental Information (NCEI). *U.S. Billion-dollar Weather and*  
593 *Climate Disasters, 1980 - present*. [https://www.ncei.noaa.gov/access/metadata/landing-](https://www.ncei.noaa.gov/access/metadata/landing-page/bin/iso?id=gov.noaa.nodc:0209268)  
594 [page/bin/iso?id=gov.noaa.nodc:0209268](https://www.ncei.noaa.gov/access/metadata/landing-page/bin/iso?id=gov.noaa.nodc:0209268) (accessed 2022-08-10).
- 595 (2) Sun, Y.; Wong, A. K. C.; Kamel, M. S. Classification of Imbalanced Data: A Review. *Int. J.*  
596 *Pattern Recognit. Artif. Intell.* **2009**, *23* (04), 687–719.  
597 <https://doi.org/10.1142/S0218001409007326>.
- 598 (3) Ho, C.-H.; Bhaduri, M. On a Novel Approach to Forecast Sparse Rare Events: Applications  
599 to Parkfield Earthquake Prediction. *Nat. Hazards* **2015**, *78* (1), 669–679.  
600 <https://doi.org/10.1007/s11069-015-1739-1>.
- 601 (4) Blair, G. S.; Henrys, P.; Leeson, A.; Watkins, J.; Eastoe, E.; Jarvis, S.; Young, P. J. Data  
602 Science of the Natural Environment: A Research Roadmap. *Front. Environ. Sci.* **2019**, *7*  
603 (121). <https://doi.org/10.3389/fenvs.2019.00121>.
- 604 (5) Wikelski, M.; Mueller, U.; Scocco, P.; Catorci, A.; Desinov, L. V.; Belyaev, M. Y.; Keim, D.;  
605 Pohlmeier, W.; Fechteler, G.; Martin Mai, P. Potential Short-Term Earthquake Forecasting  
606 by Farm Animal Monitoring. *Ethology* **2020**, *126* (9), 931–941.  
607 <https://doi.org/10.1111/eth.13078>.
- 608 (6) Xu, Y.; Vaughn, N. R.; Knapp, D. E.; Martin, R. E.; Balzotti, C.; Li, J.; Foo, S. A.; Asner, G.  
609 P. Coral Bleaching Detection in the Hawaiian Islands Using Spatio-Temporal Standardized  
610 Bottom Reflectance and Planet Dove Satellites. *Remote Sens.* **2020**, *12* (19), 3219.  
611 <https://doi.org/10.3390/rs12193219>.
- 612 (7) Izadi, M.; Sultan, M.; Kadiri, R. E.; Ghannadi, A.; Abdelmohsen, K. A Remote Sensing and  
613 Machine Learning-Based Approach to Forecast the Onset of Harmful Algal Bloom. *Remote*  
614 *Sens.* **2021**, *13* (19), 3863. <https://doi.org/10.3390/rs13193863>.
- 615 (8) Searcy, R. T.; Boehm, A. B.; Weinstock, C.; Preston, C. M.; Jensen, S.; Roman, B.; Birch, J.  
616 M.; Scholin, C. A.; Van Houtan, K. S.; Kiernan, J. D.; Yamahara, K. M. High-Frequency and  
617 Long-Term Observations of EDNA from Imperiled Salmonids in a Coastal Stream: Temporal  
618 Dynamics, Relationships with Environmental Factors, and Comparisons with Conventional  
619 Observations. *Environ. DNA* **2022**, *4* (4), 776–789. <https://doi.org/10.1002/edn3.293>.
- 620 (9) Truelove, N. K.; Patin, N. V.; Min, M.; Pitz, K. J.; Preston, C. M.; Yamahara, K. M.; Zhang,  
621 Y.; Raanan, B. Y.; Kieft, B.; Hobson, B.; Thompson, L. R.; Goodwin, K. D.; Chavez, F. P.  
622 Expanding the Temporal and Spatial Scales of Environmental DNA Research with  
623 Autonomous Sampling. *Environ. DNA* **2022**, *4* (4), 972–984.

- 624 <https://doi.org/10.1002/edn3.299>.
- 625 (10) Chan, S. N.; Thoe, W.; Lee, J. H. W. Real-Time Forecasting of Hong Kong Beach Water  
626 Quality by 3D Deterministic Model. *Water Res.* **2013**, *47* (4), 1631–1647.  
627 <https://doi.org/10.1016/j.watres.2012.12.026>.
- 628 (11) Panda, U. S.; Pradhan, U. K.; Kumar, S. S.; Naik, S.; Begum, M.; Mishra, P.; Murthy, M.  
629 V. R. Bathing Water Quality Forecast for Chennai Coastal Waters. *J. Coast. Res.* **2020**, *89*  
630 (sp1), 111–117. <https://doi.org/10.2112/SI89-019.1>.
- 631 (12) Le, X.-H.; Ho, H. V.; Lee, G.; Jung, S. Application of Long Short-Term Memory (LSTM)  
632 Neural Network for Flood Forecasting. *Water* **2019**, *11* (7), 1387.  
633 <https://doi.org/10.3390/w11071387>.
- 634 (13) Freeman, B. S.; Taylor, G.; Gharabaghi, B.; Thé, J. Forecasting Air Quality Time Series  
635 Using Deep Learning. *J. Air Waste Manag. Assoc.* **2018**, *68* (8), 866–886.  
636 <https://doi.org/10.1080/10962247.2018.1459956>.
- 637 (14) Srivastava, V.; Griess, V. C.; Padalia, H. Mapping Invasion Potential Using Ensemble  
638 Modelling. A Case Study on Yushania Maling in the Darjeeling Himalayas. *Ecol. Model.*  
639 **2018**, *385*, 35–44. <https://doi.org/10.1016/j.ecolmodel.2018.07.001>.
- 640 (15) Cruz, R. C.; Reis Costa, P.; Vinga, S.; Krippahl, L.; Lopes, M. B. A Review of Recent  
641 Machine Learning Advances for Forecasting Harmful Algal Blooms and Shellfish  
642 Contamination. *J. Mar. Sci. Eng.* **2021**, *9* (3), 283. <https://doi.org/10.3390/jmse9030283>.
- 643 (16) Shan, K.; Ouyang, T.; Wang, X.; Yang, H.; Zhou, B.; Wu, Z.; Shang, M. Temporal  
644 Prediction of Algal Parameters in Three Gorges Reservoir Based on Highly Time-Resolved  
645 Monitoring and Long Short-Term Memory Network. *J. Hydrol.* **2022**, *605*, 127304.  
646 <https://doi.org/10.1016/j.jhydrol.2021.127304>.
- 647 (17) Ömer Faruk, D. A Hybrid Neural Network and ARIMA Model for Water Quality Time  
648 Series Prediction. *Eng. Appl. Artif. Intell.* **2010**, *23* (4), 586–594.  
649 <https://doi.org/10.1016/j.engappai.2009.09.015>.
- 650 (18) Heal the Bay. *Annual Beach Report Card 2020*.  
651 <https://healthebay.org/beachreportcard2020/> (accessed 2020-10-28).
- 652 (19) Kim, J. H.; Grant, S. B. Public Mis-Notification of Coastal Water Quality: A Probabilistic  
653 Evaluation of Posting Errors at Huntington Beach, California. *Environ. Sci. Technol.* **2004**,  
654 *38* (9), 2497–2504. <https://doi.org/10.1021/es034382v>.
- 655 (20) Avila, R.; Horn, B.; Moriarty, E.; Hodson, R.; Moltchanova, E. Evaluating Statistical  
656 Model Performance in Water Quality Prediction. *J. Environ. Manage.* **2018**, *206*, 910–919.  
657 <https://doi.org/10.1016/j.jenvman.2017.11.049>.

- 658 (21) Brooks, W.; Corsi, S.; Fienen, M.; Carvin, R. Predicting Recreational Water Quality  
659 Advisories: A Comparison of Statistical Methods. *Environ. Model. Softw.* **2016**, *76*, 81–94.  
660 <https://doi.org/10.1016/j.envsoft.2015.10.012>.
- 661 (22) Francy, D. Use of Predictive Models and Rapid Methods to Nowcast Bacteria Levels at  
662 Coastal Beaches. *Aquat. Ecosyst. Health Manag.* **2009**, *12* (2), 177–182.
- 663 (23) Thoe, W.; Gold, M.; Griesbach, A.; Grimmer, M.; Taggart, M. L.; Boehm, A. B. Sunny  
664 with a Chance of Gastroenteritis: Predicting Swimmer Risk at California Beaches. *Environ.*  
665 *Sci. Technol.* **2015**, *49* (1), 423–431. <https://doi.org/10.1021/es504701j>.
- 666 (24) Francy, D. S.; Brady, A. M. G.; Cicale, J. R.; Dalby, H. D.; Stelzer, E. A. Nowcasting  
667 Methods for Determining Microbiological Water Quality at Recreational Beaches and  
668 Drinking-Water Source Waters. *J. Microbiol. Methods* **2020**, 105970.  
669 <https://doi.org/10.1016/j.mimet.2020.105970>.
- 670 (25) Searcy, R. T.; Taggart, M.; Gold, M.; Boehm, A. B. Implementation of an Automated  
671 Beach Water Quality Nowcast System at Ten California Oceanic Beaches. *J. Environ.*  
672 *Manage.* **2018**, *223*, 633–643. <https://doi.org/10.1016/j.jenvman.2018.06.058>.
- 673 (26) Thoe, W.; Lee, J. H. W. Daily Forecasting of Hong Kong Beach Water Quality by  
674 Multiple Linear Regression Models. *J. Environ. Eng.* **2014**, *140* (2), 04013007.  
675 [https://doi.org/10.1061/\(ASCE\)EE.1943-7870.0000800](https://doi.org/10.1061/(ASCE)EE.1943-7870.0000800).
- 676 (27) Vijayashanthar, V.; Qiao, J.; Zhu, Z.; Entwistle, P.; Yu, G. Modeling Fecal Indicator  
677 Bacteria in Urban Waterways Using Artificial Neural Networks. *J. Environ. Eng.* **2018**, *144*  
678 (6), 05018003. [https://doi.org/10.1061/\(ASCE\)EE.1943-7870.0001377](https://doi.org/10.1061/(ASCE)EE.1943-7870.0001377).
- 679 (28) Palani, S.; Liong, S.-Y.; Tkalich, P. An ANN Application for Water Quality Forecasting.  
680 *Mar. Pollut. Bull.* **2008**, *56* (9), 1586–1597. <https://doi.org/10.1016/j.marpolbul.2008.05.021>.
- 681 (29) Frick, W. E.; Ge, Z. F.; Zepp, R. G. Nowcasting and Forecasting Concentrations of  
682 Biological Contaminants at Beaches: A Feasibility and Case Study. *Environ. Sci. Technol.*  
683 **2008**, *42* (13), 4818–4824. <https://doi.org/10.1021/es703185p>.
- 684 (30) Zhang, J.; Qiu, H.; Li, X.; Niu, J.; Nevers, M. B.; Hu, X.; Phanikumar, M. S. Real-Time  
685 Nowcasting of Microbiological Water Quality at Recreational Beaches: A Wavelet and  
686 Artificial Neural Network-Based Hybrid Modeling Approach. *Environ. Sci. Technol.* **2018**, *52*  
687 (15), 8446–8455. <https://doi.org/10.1021/acs.est.8b01022>.
- 688 (31) Kim, S.; Mehrotra, R.; Kim, S.; Sharma, A. Probabilistic Forecasting of Cyanobacterial  
689 Concentration in Riverine Systems Using Environmental Drivers. *J. Hydrol.* **2021**, *593*,  
690 125626. <https://doi.org/10.1016/j.jhydrol.2020.125626>.
- 691 (32) Ma, J.; Cheng, J. C. P.; Lin, C.; Tan, Y.; Zhang, J. Improving Air Quality Prediction

- 692 Accuracy at Larger Temporal Resolutions Using Deep Learning and Transfer Learning  
693 Techniques. *Atmos. Environ.* **2019**, *214*, 116885.  
694 <https://doi.org/10.1016/j.atmosenv.2019.116885>.
- 695 (33) Cyterski, M.; Zhang, S.; White, E.; Molina, M.; Wolfe, K.; Parmar, R.; Zepp, R. Temporal  
696 Synchronization Analysis for Improving Regression Modeling of Fecal Indicator Bacteria  
697 Levels. *Water. Air. Soil Pollut.* **2012**, *223* (8), 4841–4851. [https://doi.org/10.1007/s11270-](https://doi.org/10.1007/s11270-012-1240-3)  
698 [012-1240-3](https://doi.org/10.1007/s11270-012-1240-3).
- 699 (34) Boehm, A. B.; Grant, S. B.; Kim, J. H.; Mowbray, S. L.; McGee, C. D.; Clark, C. D.;  
700 Foley, D. M.; Wellman, D. E. Decadal and Shorter Period Variability of Surf Zone Water  
701 Quality at Huntington Beach, California. *Environ. Sci. Technol.* **2002**, *36* (18), 3885–3892.  
702 <https://doi.org/10.1021/es020524u>.
- 703 (35) Wayne. *CA Assembly Bill 411: Beach Sanitation: Posting.*; 1997.
- 704 (36) National Oceanographic and Atmospheric Administration (NOAA). *Tide Prediction Error*  
705 *for the United States Stations*.  
706 [https://tidesandcurrents.noaa.gov/pdf/Tide\\_Prediction\\_Error\\_for\\_the\\_United\\_States\\_Coastli](https://tidesandcurrents.noaa.gov/pdf/Tide_Prediction_Error_for_the_United_States_Coastline.pdf)  
707 [ne.pdf](https://tidesandcurrents.noaa.gov/pdf/Tide_Prediction_Error_for_the_United_States_Coastline.pdf) (accessed 2022-08-17).
- 708 (37) Pedregosa, F.; Varoquaux, G.; Gramfort, A.; Michel, V.; Thirion, B.; Grisel, O.; Blondel,  
709 M.; Prettenhofer, P.; Weiss, R.; Dubourg, V.; Vanderplas, J.; Passos, A.; Cournapeau, D.;  
710 Brucher, M.; Perrot, M.; Duchesnay, É. Scikit-Learn: Machine Learning in Python. *J. Mach.*  
711 *Learn. Res.* **2011**, *12* (85), 2825–2830.
- 712 (38) Searcy, R. T.; Boehm, A. B. *Data for FIB Forecasting Project*. Stanford Digital  
713 Repository. <https://purl.stanford.edu/nw799cp6263> (accessed 2022-08-15).
- 714 (39) Thoe, W.; Gold, M.; Griesbach, A.; Grimmer, M.; Taggart, M. L.; Boehm, A. B. Predicting  
715 Water Quality at Santa Monica Beach: Evaluation of Five Different Models for Public  
716 Notification of Unsafe Swimming Conditions. *Water Res.* **2014**, *67*, 105–117.  
717 <https://doi.org/10.1016/j.watres.2014.09.001>.
- 718 (40) Naloufi, M.; Lucas, F. S.; Souihi, S.; Servais, P.; Janne, A.; Wanderley Matos De Abreu,  
719 T. Evaluating the Performance of Machine Learning Approaches to Predict the Microbial  
720 Quality of Surface Waters and to Optimize the Sampling Effort. *Water* **2021**, *13* (18), 2457.  
721 <https://doi.org/10.3390/w13182457>.
- 722 (41) Xu, T.; Coco, G.; Neale, M. A Predictive Model of Recreational Water Quality Based on  
723 Adaptive Synthetic Sampling Algorithms and Machine Learning. *Water Res.* **2020**, 115788.  
724 <https://doi.org/10.1016/j.watres.2020.115788>.
- 725 (42) Park, Y.; Kim, M.; Pachepsky, Y.; Choi, S.-H.; Cho, J.-G.; Jeon, J.; Cho, K. H.

- 726 Development of a Nowcasting System Using Machine Learning Approaches to Predict Fecal  
727 Contamination Levels at Recreational Beaches in Korea. *J. Environ. Qual.* **2018**.  
728 <https://doi.org/10.2134/jeq2017.11.0425>.
- 729 (43) Searcy, R. T.; Boehm, A. B. A Day at the Beach: Enabling Coastal Water Quality  
730 Prediction with High-Frequency Sampling and Data-Driven Models. *Environ. Sci. Technol.*  
731 **2021**, *55* (3), 1908–1918. <https://doi.org/10.1021/acs.est.0c06742>.
- 732 (44) Madani, M.; Seth, R. Evaluating Multiple Predictive Models for Beach Management at a  
733 Freshwater Beach in the Great Lakes Region. *J. Environ. Qual.* **2020**, *49* (4), 896–908.  
734 <https://doi.org/10.1002/jeq2.20107>.
- 735 (45) Boehm, A. B.; Lluch-Cota, D. B.; Davis, K. A.; Winant, C. D.; Monismith, S. G.  
736 Covariation of Coastal Water Temperature and Microbial Pollution at Interannual to Tidal  
737 Periods. *Geophys. Res. Lett.* **2004**, *31* (6). <https://doi.org/10.1029/2003GL019122>.
- 738 (46) Olyphant, G. A.; Whitman, R. L. Elements of a Predictive Model for Determining Beach  
739 Closures on a Real Time Basis: The Case of 63rd Street Beach Chicago. *Environ. Monit.*  
740 *Assess.* **2004**, *98* (1–3), 175–190. <https://doi.org/10.1023/B:EMAS.0000038185.79137.b9>.
- 741 (47) Desai, A. M.; Rifai, H. S. Escherichia Coli Concentrations in Urban Watersheds Exhibit  
742 Diurnal Sag: Implications for Water-Quality Monitoring and Assessment. *J. Am. Water*  
743 *Resour. Assoc.* **2013**, *49* (4), 766–779. <https://doi.org/10.1111/jawr.12039>.
- 744 (48) Qin, M.; Li, Z.; Du, Z. Red Tide Time Series Forecasting by Combining ARIMA and Deep  
745 Belief Network. *Knowl.-Based Syst.* **2017**, *125*, 39–52.  
746 <https://doi.org/10.1016/j.knosys.2017.03.027>.
- 747 (49) Lucius, N.; Rose, K.; Osborn, C.; Sweeney, M. E.; Chesak, R.; Beslow, S.; Schenk, T.  
748 Predicting E. Coli Concentrations Using Limited QPCR Deployments at Chicago Beaches.  
749 *Water Res. X* **2019**, *2*, 100016. <https://doi.org/10.1016/j.wroa.2018.100016>.
- 750 (50) Yamahara, K. M.; Demir-Hilton, E.; Preston, C. M.; Marin, R.; Pargett, D.; Roman, B.;  
751 Jensen, S.; Birch, J. M.; Boehm, A. B.; Scholin, C. A. Simultaneous Monitoring of Faecal  
752 Indicators and Harmful Algae Using an In-Situ Autonomous Sensor. *Lett. Appl. Microbiol.*  
753 **2015**, *61* (2), 130–138. <https://doi.org/10.1111/lam.12432>.